# 3D FIELD COMPUTATIONS FOR MAIN PROTOTYPE MAGNETS OF THE SIS100 ACCELERATOR OF THE FAIR PROJECT

P. Shcherbakov, IHEP, Protvino, Russia
E. Fischer, GSI, Darmstadt, Germany,
R. Kurnyshov, Electroplant, Moscow, Russia.

*Abstract*

Fast cycling superferric magnets will be used for the new international accelerator Facility for Antiprotons and Ion Research (FAIR) at GSI, Darmstadt. The dipoles and quadrupoles have to provide the required field quality from the injection field of 0.25T and 4.3T/m up to the maximum values of 2.1T and 35T/m respectively. The complex 3D magnetic field distribution, due to the longitudinal component $B_z$ near the end regions of the yoke and due to the presence of eddy currents in the bulk construction elements as well as in a mechanical stable beam pipe, can create unacceptable static and dynamic nonlinearities. An in detail understanding of these effects is necessary to control the field quality for all operating cycles to be provided by the SIS100 accelerator. We discuss the methodical problems of 3D finite element calculations (ANSYS) of the local and the integral nonlinearities, considering also the problems caused by the various nonlinear and anisotropic material properties and by the structure elements of the yoke and beam pipe. The calculated integral harmonics are presented for the static case and the case affected by eddy currents.

## INTRODUCTION

In the accelerator magnet design ANSYS is mainly used for structural and thermal problems. The application of this powerful code on electromagnetic problems is limited. In particular, it is usually used for 2D and 3D static calculations of accelerator magnets [1,2,3]. In our previous paper [4] the results of transient process calculations in short models of SIS100 dipoles and quadrupoles have been presented together with a comparison with calorimetric AC loss measurements. It was shown that the complex 3D geometry of accelerator magnets, including laminated electric steel, bulk restraint elements of the end plates (EP) of the yoke (Y) assembly, long brackets (BR), cooling tubes and the beam pipe (BP), can be successfully calculated by ANSYS for static as well transient processes in all the aforementioned parts of the magnet. It allowed us to calculate the hysteresis and eddy current components of the AC losses in each part of the magnet and distinguish the contribution of different components of the magnet to the total calorimetricaly measured value. This permitted to control the effect of design modifications during magnet development (change of material, reducing the mass, slits, cuts). Now the model is extended to the real full scale prototype and to calculating the magnetic field, its homogeneity and AC losses for the static and the dynamic cases.

## FULL SCALE DIPOLE

***Design geometry.*** The main parameters and figures of full scale magnet design are presented in status paper on SIS100 magnets [5]. Fig.1. shows the end part of the dipole. The features are: Rogovsky profile, 3 longitudinal end slits of 200 mm length in laminated yoke, end plates and brackets from stainless steel, the formers have long holes. All design features of the magnet are essential and cannot be neglected for precise calculations: the horizontal end slits reduce the effective plane $\mu_{xy}$ (like laminations reduce longitudinal $\mu_z$), the Rogovski profile reduces saturation, but reduces the effective length. The end plates and brackets made of stainless steel reduce AC losses, but decrease the effective length and the thickness of the yoke, affecting the field quality, especially at high field level.

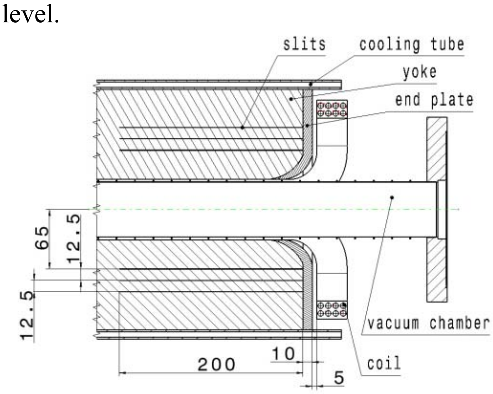


Figure 1: End parts of the yoke assembly and the coil.

The model has been created with these 2D and 3D features of the magnet assembly to calculate simultaneously AC losses and field quality in the transient processes for arbitrary cycles and for sequences with plateau and pauses. It is shown in Fig.2. It allowed us to calculate the 3D static field and the hysteresis losses in the yoke asembly as well as the more difficult problem of the field and eddy current losses at operating dB/dt.

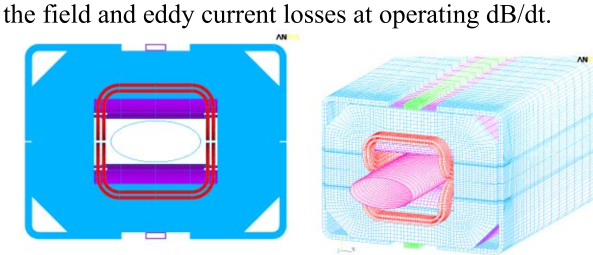

Figure 2: Front layout of SIS100 prototype dipole: yoke end part profile, coil end parts reinforced brackets, cooling pipe, beam pipe.

*Steel properties*. The magnetic properties of electrical steel have been reported in [4]. The anisotropy of the magnetic properties of laminated steel is taken into account using a constant permeability in the z direction. Up to 1.6 T, depending on packing factor $f_p$ , the usually used nonlinear dependence is constant. So this approach gives a good approximation of a nonlinear dependence. The permeability of stainless steel of the vacuum chamber is 1.005. The electrical resistivity at 4.2 K was taken as 0.31 μΩ·m and 0.5 μΩ·m for the electrical steel and stainless steel respectively.

## METHODICAL PROBLEMS

For the static and transient calculations magnetic edge elements have been used, defining the relative magnetic potential.The aim of meshing was to solve the complex problem of calculating the AC losses and the field quality for the real 3 m long magnet design (Y+Br+EP+BP) in cycles with f=1 Hz and $B_{max}$=2.1 T in acceptable time using only one mesh.. The features of the cross section and the longitudinal design result in an increased number of elements in 2D. The chamfering or Rogovsky profile of the slitted body together with the end plate and beam tube flange necessitates an increased number of volume elements. Careful meshing has been carried out providing consistent results for the field harmonics (coefficients of $B_r$ and $B_{\square}$, radial dependence) in the central section of the magnet for the 2D and 3D models. Different elements, their density, point numbers and placements have been tested with criteria of equality of the coefficients for $B_r$ and $B_\theta$, radial dependence and equality to zero of even and scew coefficients up to $10^{-12}$ for the dipole.

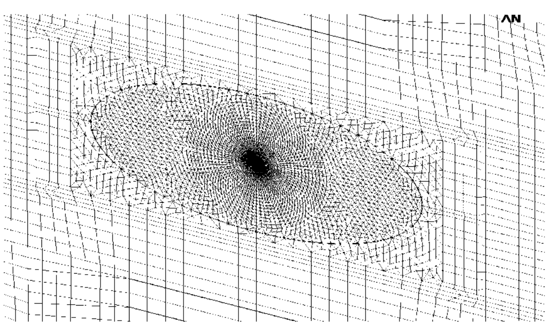

Figure 3: Mesh in the aperture.

The mesh in 3D has been tested concerning the harmonic coefficients and homogeneity with help of 2D simulation. The mesh producing the best agreement of the 2D and 3D harmonic was selected (see Fig.3). The mesh in the aperture of the dipole is formed by triangular prisms.

## RESULTS

### *Static 3D Field Distributions*

The distributions of the absolute magnetic field value B is shown in Fig. 4. The harmonic coefficients of the central and integrated field at r=20 mm (without beam pipe) are presented in Table 1 and Table 2 for two current levels. The coefficients are small at lower fields, sharply increasing near the maximum current.

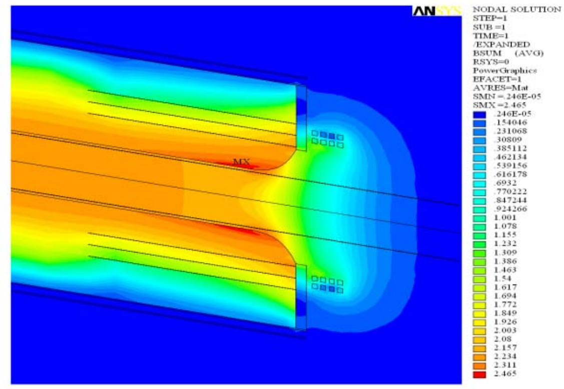

Figure 4: Distribution of the absolut field B.

Table 1: Central harmonic coefficients

| | $C_1$, T | $C_3/C_1$ | $C_5/C_1$ | $C_7/C_1$ |
|---|---|---|---|---|
| I,A | T | 10**-5 | 10**-6 | 10**-8 |
| 3850 | 1.171 | 0.33 | -1.70 | -1.9 |
| 7700 | 2.220 | 33.3 | 22.6 | 234 |

Table 2: Integral harmonic coefficients

| | $B_0$ | C | $C_3/C_1$ | $C_5/C_1$ | $C_7/C_1$ |
|---|---|---|---|---|---|
| I, A | T | T•m | $10^{-5}$ | $10^{-6}$ | $10^{-6}$ |
| 3850 | 1.171 | 3.186 | -3.24 | 5.74 | 1.33 |
| 7700 | 2.220 | 6.011 | 46.7 | 33.1 | 3.22 |

### *Hysteresis Losses*

The fields, calculated for the yoke, allow us to estimate the hysteresis loss with an accuracy, limited only by the accuracy of the measured $W_h(B)$ curve used for the steel. The distribution of the hysteresis loss in the different sections of the magnet yoke is shown in Fig.5. Losses are 32.6 W or 10.8 W/m.

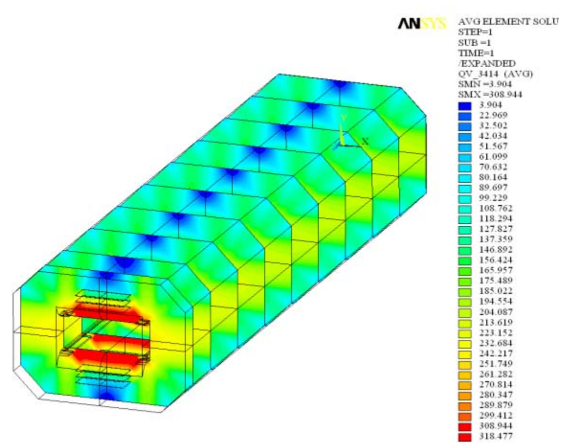

Fig. 5: Distribution of hysteresis losses in the laminated yoke.

### *3D Transient Process*

***Eddy current losses in beam pipe.*** The time dependences of the eddy current loss in the beam pipe have been calculated using $\rho_{ss}$=0.5 μΩ·m for two cycles with no plateau. The results are shown in Fig. 6 .

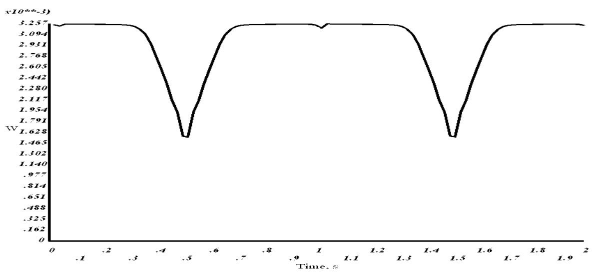

Figure 6: AC loss power in a stainless steel tube (0.5 mm).

The normalized loss of the tube is 5.96 W/m. It is close to analytical results with dB/dt=const, but our case is correct for real dB(t)/dt, depending on saturation. The total loss in the yoke assembly (no beam pipe) in the standard cycle is 12-14 W/m

***Harmonics***. Previous calculations for short dipole model with elements from low carbon steel showed that their eddy currents can add about $10^{-4}$ to static harmonic $C_3$ at r=25 mm.

Full scale dipole use only stainless steel for brackets and endplates. The main artifacts are created in this case by the beam tube. Big eddy currents cause big AC losses and disturb the field quality.

## FULL SCALE QUADRUPOLE

The quadrupole design is described in status report [5]. The features are: slitted laminations and shamfering of the end parts of the yoke. The mesh is presented in Fig. 7

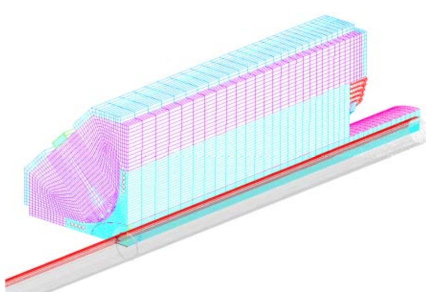

Fig. 7: Mesh for the quadrupole (including beam pipe) with pathes for the calculation of the integrated static and transient harmonics.

The hysteresis and eddy current losses in the magnet yoke assembly and the beam pipe are presented in [5]. Here the results for the field quality are given both in static and dynamic cases. We were calculate quadrupole together with the elliptical tube 135x65 mm with thickness of 0.3 mm. At 4.2 K the permeability of stainless steel is 1.005, the resistivity is 0.5 μΩ·m.

***Static multipoles***. The static multipole coefficients in central section and integrated ones at radius of 20mm are presented in Table 3. The elliptical beam pipe creates the coefficient $C_4$ and $C_8$ due to the permeability of stainless steel. The central coefficients are-1.1 $10^{-5}$ and 0.98 $10^{-5}$ respectively and the integrated are 4.8 $10^{-5}$ and 1.47 $10^{-5}$.

Table 3: The central and integrated normalized coefficients (with elliptic beam pipe) for two current levels.

| | Central coefficients | | | Integrated | | |
|---|---|---|---|---|---|---|
| I, A | $C_2$, T | $C_{6n}$, $^{5}$ | $C_{10n}$, $10^{-5}$ | $C_{2i}$, T•m | $C_{6in}$, $10^{-5}$ | $C_{10in}$, $10^{--6}$ |
| 4000 | .4006 | -2.19 | 4.0 | 4.125 | -1.56 | 2.33 |
| 8000 | .6520 | -1.63 | 4.09 | 6.598 | -6.39 | -1.55 |

***Multipoles in transient processes***. The coefficients $C_6$ and $C_{10}$ of the central and integrated field obtained at r=2 cm are affec-ted by the transient process. The elliptical beam pipe creates the multipoles due to eddy currents. The integrated $C_4$ and $C_8$ are 4.3 $10^{-5}$ and 1.36 $10^{-5}$ respectively, including the static influence of the stainless steel pipe. The transient process calculations had showen, that the effect of eddy current loss in all elements of the yoke assembly is small and the eddy current do not affect the field quality in the aperture, but the elliptic tube with $\mu$ = 1.005 does not only create additional static coefficients ($C_4$ and $C_8$), but the eddy currents disturb also the dynamical field in the aperture.

## CONCLUSION

The precise 3D calculation of static and transient processes has been successfully carried out for full scale SIS100 prototype dipoles with different 2D and 3D features within the limits of our hardware. It is confirmed, that with the help of ANSYS and the well known CAD codes, an experienced magnet designer can solve all design aspects (magnetic, thermal and mechanical). It is not ultimative necessary to use other commercial codes to calculate the fields, losses and forces. Excellent CAD software and ANSYS together with comfortable pre and post processing permits fast feedback to the magnet design.

## REFERENCES

[1] D. Johnson, T.Kio and F.Marti "Calculation of 3D magnetic fields with ANSYS, a finite element commercial code" , proc. of EPAC-92., p.p. 939-941.

[2] A. Koski, R. Bandelmann and S.Wolf, "Superconducting Magnet Package for the TESLA TEST Facility, DESY 95-23, Sept 1995, MT-14, Finland, June , 1995

[3] L.R. Turner, "3D field computation: near-triumph of commercial codes", IEEE Trans. on Magnetics, Vol.32 (4), pp. 2945–2949, July 1996.

[4] E. Fischer et al.., "3D transient process calculations for fast cycling superferric accelerator magnet", MT-19, THA07PO06

[5] A. Kovalenko et al., "Full length superferric dipole and quadrupole prototype magnets for the SIS100 at GSI: status of the design and manifacturing", EPAC'2006, WEPLS090